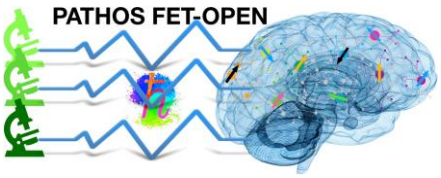

European Commission

PHOTONIC AND NANOMETRIC HIGH-SENSITIVITY BIO-SENSING

DELIVERABLE 3.1 [HUJI, M30]
REPORT ON THE DEMONSTRATION OF HIGH-RESOLUTION NV OPTICAL IMAGING WITH CS

WEIZMANN INSTITUTE OF SCIENCE
INRiM ISTITUTO NAZIONALE DI RICERCA METROLOGICA
technische universität dortmund
THE HEBREW UNIVERSITY OF JERUSALEM

ENHANCED NV MAGNETIC IMAGING WITH COMPRESSED SENSING

Work Package 3

John Howell and Nir Bar-Gill, Hebrew University, Jerusalem, Israel

Project number: 828946
Project partners: UNIFI, Weizmann, INRiM, HUJI, TUDO

Contents

1 Executive Summary

As part of Deliverable 3.1 [M30], we have expanded over our theory and initial results on optical compressed sensing (CS) with NVs (reported on D3.6), demonstrating the integration of compressed sensing schemes with NV magnetic imaging, to enhance the overall sensitivity, bandwidth, dynamic range, and resolution.

The experimental results presented here demonstrate the advantages of NV magnetic sensing and imaging using compressed sensing, specifically for large signal scenarios. Based on this report, and following final measurements and analysis, the results will be summarized and sent for publication.

2 Introduction

2.1 NV magnetic sensing

NV magnetic sensing has already been established as a useful technique in various scenario, leveraging the robustness of the diamond sensor (enabling operation at ambient conditions as well as in harsh environments) along with the high-resolution and high sensitivity afforded by the optical readout of the signal and the favorable coherence properties of the NV defects (see more details in reports D3.5 and D3.6).
Briefly, we realize NV magnetic sensing and imaging through a home-built magnetic microscope, depicted in Figure 1(a). An externally applied magnetic field (created here using Helmholtz coils) lifts the degeneracy of the NV's $m_s = \pm 1$ spin states (b). In a sensing/imaging scenario in which an ensemble of NVs is interrogated, all 4 possible NV lattice orientations, shown in (c), are measured. This results in an optically detected magnetic resonance signal (d), with 4 pairs of resonances observed through the change of the fluorescence signal as a function of the frequency of the applied microwave drive.

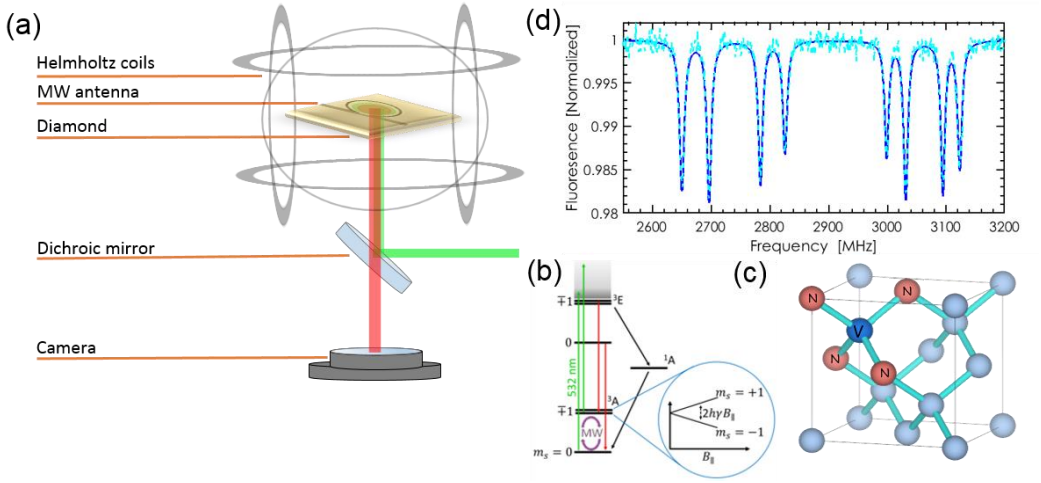

Figure 1: (a) Experimental setup schematic, NV's are excited with green laser, manipulated with MW, and red fluorescence is imaged onto a sCMOS camera, in an Epi-illumination scheme. Helmholtz coils generate a magnetic field to distinguish between the resonances of the different orientations. (b) NV center's electronic energy levels, ground state degeneracy is lifted due to Zeeman shift. (c) The diamond lattice structure with the 4 allowed NV orientations. (d) ESR spectrum of NV ensemble, 8 resonances correspond to $m_s = \pm 1$ of each orientation.

Standard NV magnetic sensing and imaging is based on extracting the precise location of the resonances, as described in D3.5. While this is a useful and well-established approach, it could be prohibitively time consuming to sample many microwave frequency points to pinpoint the resonance locations, especially in high magnetic field situations (requiring a large frequency range to be swept). This limitation translates into reduced sensitivity, bandwidth and dynamic range. We note that in most scenarios and in the values quoted for magnetic sensitivity in the literature, it is assumed that a small signal regime is relevant, such that the spectral locations of the resonances are roughly known, and only measuring small deviations from them are required, such that only a couple of measurements on the slope of each resonance are needed.
Here we focus on the large signal regime, which is relevant for unknown fields with potentially non-negligible gradients, and for which the standard approach inevitably leads to large frequency sweeps that translate into the limitations mentioned above. In such cases, an advanced compressed sensing approach can significantly enhance magnetic sensing performance metrics.

2.2 Compressed sensing in magnetic resonance

The concept and theory behind enhanced compressed magnetic sensing with NVs was presented in D3.6.
In brief, we observe that the identification of the resonance locations in frequency space, which usually entails a long frequency sweep across the relevant range, can be formulated as a sparse measurement with a Lorentzian resonance shape basis. As such, it can benefit from the concepts of compressed sensing – we have analyzed this problem theoretically and have shown that iterative measurements in which more than one microwave frequency is applied at a time, can converge with high sensitivity much faster than standard raster scanning (D3.6).

In our experiment the bias magnetic field determines the window over which we expect frequencies to occur. Define this set of M frequencies $\{\nu_j\}_{j=1}^{M}$ at which we may measure and define the set of frequencies $\{\nu_k\}_{k=1}^{N}$ as those locations where we allow for the possibility that a resonance is present. We can write the total lineshape as a linear combination of Lorentzians centered at the resonance locations.
Our procedure is as follows: we first sample at a number of frequencies across *all* ν_j. The choice of which frequencies we apply is saved in a M-column sampling matrix, each row corresponds to a single projection with entries corresponding to the random frequencies chosen and zeros if that microwave frequency was not chosen at all. We run a measurement on the chosen frequencies and attempt to reconstruct the data. After each reconstruction we check whether 8 peaks were found, if the answer is no, the algorithm continues to another measurement with other random frequencies. Once these peak locations have converged, the data is fitted, and the reconstruction parameters are used as an initial guess for the next run. After four consecutive measurements found identical (within some pre-determined error), the code breaks the loop.
We use total variation minimization, specifically the algorithm provided by the L1 minimization, to reconstruct our 1D signal at each reconstruction step.

We note that the iterative method of compressed sensing converges to the correct answer with a finite probability of success. We therefore consistently derive a sensitivity measure that includes the probability of success, such that a fair comparison can be made between CS and raster scanning:

$$\eta = \delta B \sqrt{\frac{T}{p}}$$

Where η is the sensitivity in units of $Gauss/\sqrt{Hz}$, δB is the measured uncertainty in the field (i.e. in the resonance positions), T is the measurement (averaging) time, and p is the success probability.

3 NV compressed magnetic sensing results

3.1 Enhanced sensitivity

We implemented the CS algorithm into our NV magnetic sensing platform, and compared the resulting magnetic sensitivity as a function of the number of measurements taken. This can be translated into the corresponding sub-sampling of a regular raster scan, or to a limited repetition of the iterative CS scheme. This analysis is useful as it provides a fair comparison between the CS and regular raster scanning techniques, and demonstrates the achievable optimum in terms of the compromise between the number of measurements (measurement time) and the desired sensitivity.
In Figure 2 we present the simulation results for a magnetic measurement at a field of $B{\sim}120G$, in terms of the sensitivity as a function of the number of measurements, comparing raster scanning (red stars) to CS with different numbers of simultaneous microwave frequencies applied (dots – blue for 2 frequencies, red for 3 frequencies and green for 4 frequencies). It is clear that CS displays an advantage for nearly all scenarios, with special emphasis on fast (few measurement, less than ~100) scans, for which the raster sub-sampling completely fails, while the CS provides adequate results.

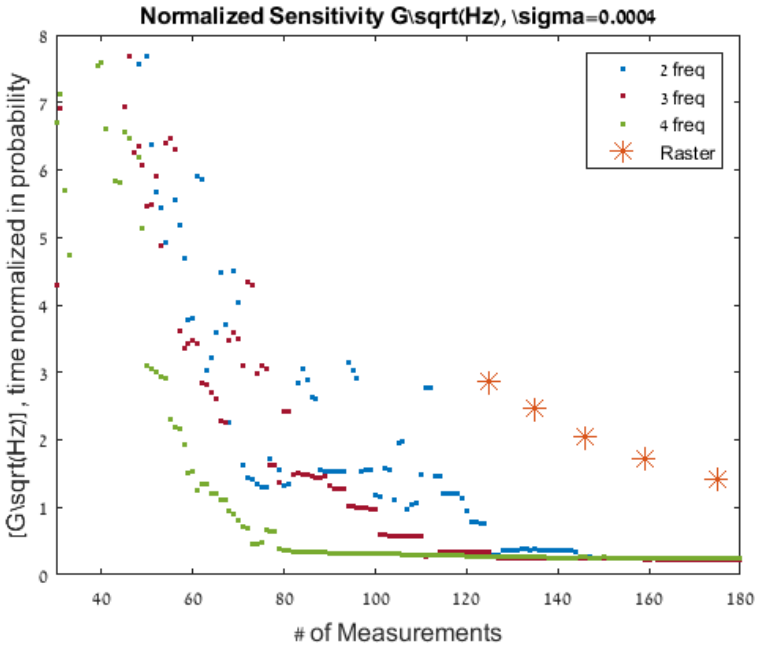

Figure 2: Comparison of magnetic sensitivity for raster scanning vs. CS. Sensitivity is plotted as a function of the number of measurements, simulated for a background field of $B = 120G$ and a measurement noise of 0.04%. The raster sub-sampling results are shown in red stars, while the CS is displayed as dots of different colors: blue for 2 simultaneous microwave frequencies, red for 3 frequencies and green for 4 frequencies.

The experimental results realizing the scenario depicted above in simulation are shown in Figure 3. Here we plot the measurement uncertainty, in terms of the extracted spectral position of the resonances, in units of MHz, as a function of the number of measurements. We clearly observe a significant advantage of the CS technique compared to raster sub-sampling, specifically for the case fast scan, i.e. few measurement (<200).
We note that the uncertainity for the CS seems to saturate rather quickly at around 100 measurements, which we don't fully understand. This is currently under investigation, and we believe can be improved through tweaking of the implementation of the CS algorithm.

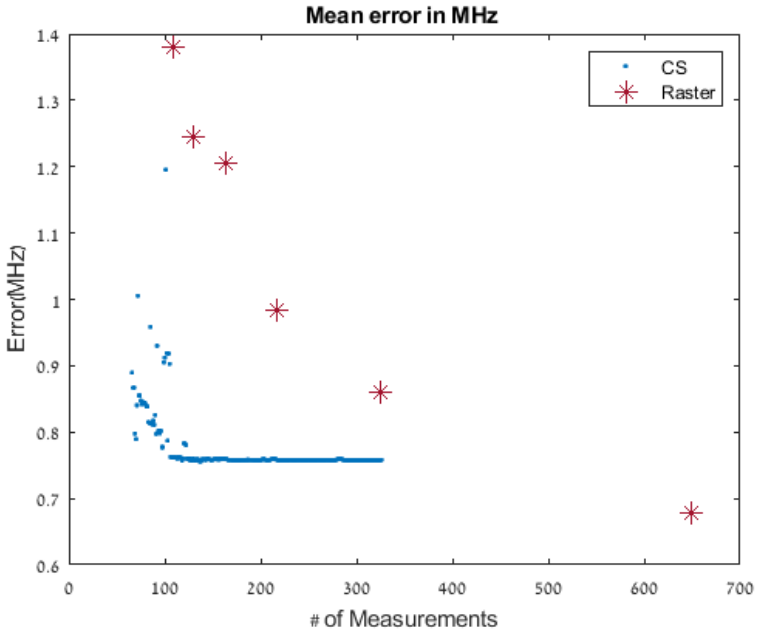

Figure 3: Measurement results comparing raster sub-sampling and CS with 2 simultaneous frequencies. As before, the background field is $B = 120G$, and the raster scan results are shown in red stars while the CS in blue dots. We plot the measurement uncertainty in MHz as a function of the number of measurements, clearly demonstrating the advantage of the CS approach, specifically for fast (few measurement) scenarios.

Similar results have been obtained for a lower background field of $B = 50G$, shown in Figure 4. Here we plot the calculated sensitivity as a function of the number of measurements, again comparing raster scans and CS. The enhanced sensitivity of the CS technique is clear, with significant improvements observed for <50 measurements.

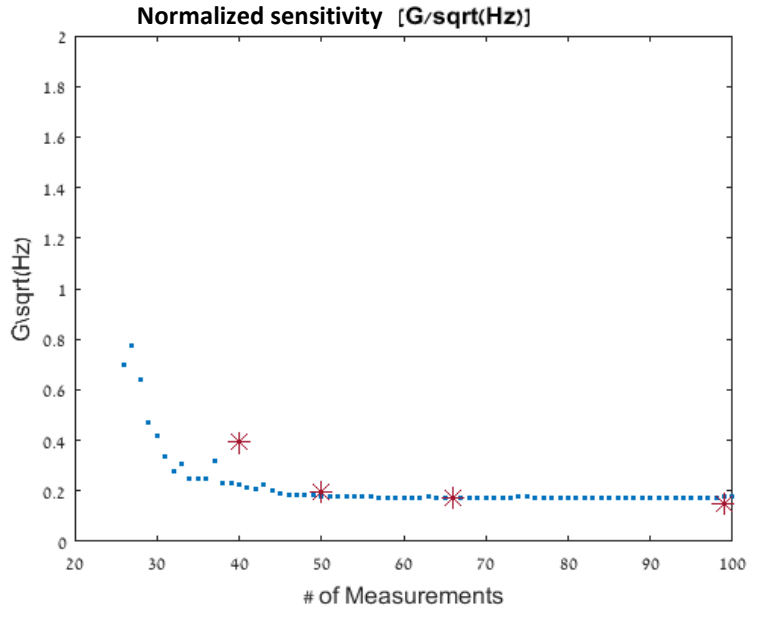

Figure 4: Measurement results comparing raster sub-sampling and CS with 2 simultaneous frequencies. The background field is $B = 50G$, and the raster scan results are shown in red stars while the CS in blue dots. We plot the overall magnetic sensitivity in $G/\sqrt{Hz}$ as a function of the number of measurements, demonstrating the advantage of CS for low numbers of measurement points.

3.2 Improved magnetic imaging

The enhanced magnetic sensing demonstrated above can be incorporated into a magnetic imaging platform, wherein for each optical pixel the CS magnetic sensing is applied. Following the previous results and discussion, this approach could be specifically significant in cases for which fast imaging is desired, and magnetic field variations across the field of view are not negligible (and thus beyond the small signal regime).
We performed a measurement in which a current-carrying wire was placed on top of the diamond sample, such that the magnetic field created by the current can be imaged. The setup is described in Figure 5.

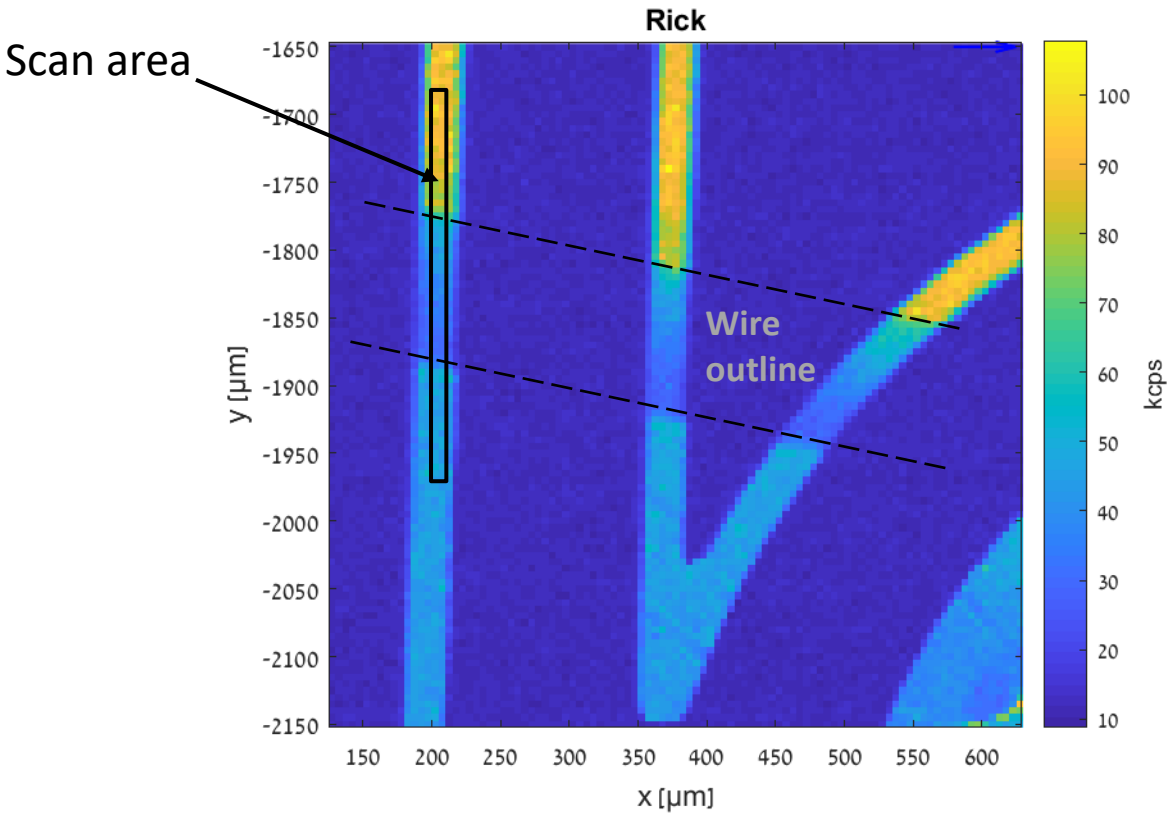

Figure 5: Optical image of the setup for CS magnetic imaging. The diamond is imaged through a micro-fabricated structure for delivering the microwave signals. The dashed black lines depict the outline of the current-carrying wire which creates the magnetic field to be measured. The measurement field of view is shown as a solid black rectangle.

We imaged the magnetic signal in the field of view with a full raster scan (of 600 measurements), while the CS imaging was performed 4 times faster (with 150 measurements). The results are presented in Figure 6. While the CS image is slightly more noisy than the full raster scan, it captures the main features of the image, demonstrating the achieved improvement in terms of bandwidth and dynamic range. We note that a similarly short measurement performed with raster sub-sampling essentially fails (does not identify the resonance positions).

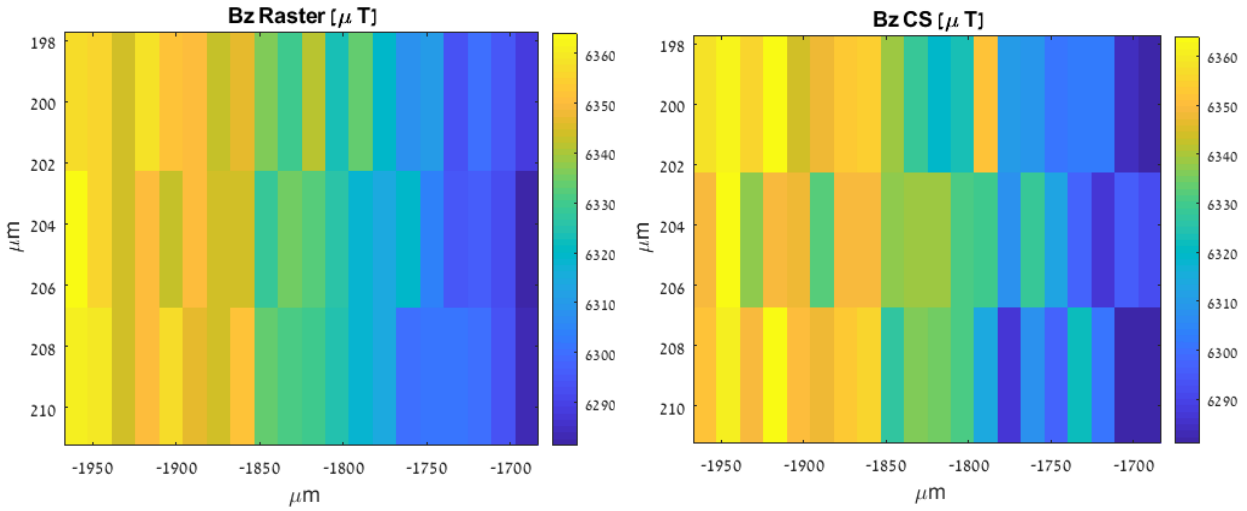

Figure 6: Magnetic field image obtained using full raster scanning (left) vs. CS (right). The magnetic field was created by a current carrying wire placed near the diamond surface. The full raster scan consisted of 600 measurement points, while the CS magnetic imaging was 4 times faster, with only 150 measurement points.

4 Future directions

We are exploiting the current collaboration between HUJI and UNIFI (specifically with the group of Filippo Caruso), to research and implement potential avenues for enhanced CS sensitivity by incorporating machine learning techniques. These directions could potentially shed light on sensitivity limits and novel analysis schemes, and possibly address remaining issues such as the noise floor observed as the plateau in Figure 3.